

DTIC FILE COPY

WRDC-TR-90-2044



AD-A222 489

SELF-LUBRICATING SURFACES BY ION BEAM PROCESSING

Rabi S. Bhattacharya

Universal Energy Systems, Inc.
4401 Dayton-Xenia Road
Dayton, OH 45432

June 1990

DTIC
ELECTE
JUN 06 1990
S D D

Final Report for Period August 1989 - March 1990

Approved for Public Release; Distribution is Unlimited

AERO PROPULSION AND POWER LABORATORY
WRIGHT RESEARCH AND DEVELOPMENT CENTER
AIR FORCE SYSTEMS COMMAND
WRIGHT-PATTERSON AIR FORCE BASE, OHIO 45433-6563

90 06 06 023

NOTICE

When Government drawings, specifications, or other data are used for any purpose other than in connection with a definitely Government-related procurement, the United States Government incurs no responsibility or any obligation whatsoever. The fact that the government may have formulated or in any way supplied the said drawings, specifications, or other data, is not to be regarded by implication, or otherwise in any manner construed, as licensing the holder, or any other person or corporation; or as conveying any rights or permission to manufacture, use, or sell any patented invention that may in any way be related thereto.

This report is releasable to the National Technical Information Service (NTIS). At NTIS, it will be available to the general public, including foreign nations.

This technical report has been reviewed and is approved for publication.



LEWIS ROSADO, Project Engineer
Lubrication Branch
Fuels and Lubrication Division
Aero Propulsion and Power Laboratory



HOWARD F. JONES, Chief
Lubrication Branch
Fuels and Lubrication Division
Aero Propulsion and Power Laboratory

FOR THE COMMANDER



BENITO P. BOTTERI, Chief
Fuels and Lubrication Division
Aero Propulsion and Power Laboratory

If your address has changed, if you wish to be removed from our mailing list, or if the addressee is no longer employed by your organization please notify WRDC/POSL, WPAFB, OH 45433-6563 to help us maintain a current mailing list.

Copies of this report should not be returned unless return is required by security considerations, contractual obligations, or notice on a specific document.

REPORT DOCUMENTATION PAGE

Form Approved
OMB No. 0704-0188

1a. REPORT SECURITY CLASSIFICATION		1b. RESTRICTIVE MARKINGS	
2a. SECURITY CLASSIFICATION AUTHORITY		3. DISTRIBUTION / AVAILABILITY OF REPORT	
2b. DECLASSIFICATION / DOWNGRADING SCHEDULE		Approved for Public Release; Distribution is Unlimited.	
4. PERFORMING ORGANIZATION REPORT NUMBER(S)		5. MONITORING ORGANIZATION REPORT NUMBER(S)	
		WRDC-TR-90-2044	
6a. NAME OF PERFORMING ORGANIZATION	6b. OFFICE SYMBOL (if applicable)	7a. NAME OF MONITORING ORGANIZATION	
Universal Energy Systems, Inc.		Aero Propulsion and Power Lab (WRDC/POSL) Wright Research and Development Center	
6c. ADDRESS (City, State, and ZIP Code)		7b. ADDRESS (City, State, and ZIP Code)	
4401 Dayton-Xenia Road Dayton, OH 45432		Wright-Patterson AFB, Oh 45433-6563	
8a. NAME OF FUNDING / SPONSORING ORGANIZATION	8b. OFFICE SYMBOL (if applicable)	9. PROCUREMENT INSTRUMENT IDENTIFICATION NUMBER	
Aero Propulsion & Power Lab		F33615-89-C-2944	
8c. ADDRESS (City, State, and ZIP Code)		10. SOURCE OF FUNDING NUMBERS	
United States Air Force Wright Research & Development Center Aeronautical Systems Division (AFSC) Wright-Patterson AFB, OH 45433-6563		PROGRAM ELEMENT NO.	PROJECT NO.
		65502F	3005
		TASK NO.	WORK UNIT ACCESSION NO.
		21	53
11. TITLE (Include Security Classification)			
Self-Lubricating Surfaces By Ion Beam Processing			
12. PERSONAL AUTHOR(S)			
Rabi S. Bhattacharya			
13a. TYPE OF REPORT	13b. TIME COVERED	14. DATE OF REPORT (Year, Month, Day)	15. PAGE COUNT
Final	FROM 08/11/89 TO 03/16/90	1990 June	34
16. SUPPLEMENTARY NOTATION			
This is a Small Business Innovative Research Program Report, Phase I			
17. COSATI CODES			18. SUBJECT TERMS (Continue on reverse if necessary and identify by block number)
FIELD	GROUP	SUB-GROUP	
			Ion Implantation, Ion Beam Assisted Deposition, Self-Lubrication, Coating, Thin Film, Si ₃ N ₄ , M50 Steel, Friction and Wear, Materials, Vapor Deposition JG
19. ABSTRACT (Continue on reverse if necessary and identify by block number)			
<p>The primary research objective of this work was to develop self-lubricating surface and coatings through direct ion implantations and a combined process of electron beam evaporation and ion implantation. The latter is most commonly referred in the literature as ion beam-assisted deposition (IBAD). IBAD of bi-layer coating of CaF₂/Ag on Si₃N₄ resulted in a very adherent coating that exhibited significantly low friction and wear characteristic at both room and elevated temperatures (800°C). Ion beam assisted TiO₂ coating on M50 steel showed significantly improved friction and wear characteristics at room temperature. Ion beam assisted CdO coating lowered the friction coefficient of M50 steel at 400°C. The ion beam-assisted deposition technique for fabricating self-lubricating surfaces appears to have good technical feasibility for defense and industrial applications, owing to the overall simplicity and scalability of the technique. The initial applications are likely to be in the seals and bearings of engines, variable stator vanes, etc., in gas turbine engine technology.</p> <p>Calcium Fluoride / Silver deq Titanium dioxide</p>			
20. DISTRIBUTION / AVAILABILITY OF ABSTRACT		21. ABSTRACT SECURITY CLASSIFICATION	
<input checked="" type="checkbox"/> UNCLASSIFIED/UNLIMITED <input type="checkbox"/> SAME AS RPT. <input type="checkbox"/> DTIC USERS		Unclassified	
22a. NAME OF RESPONSIBLE INDIVIDUAL	22b. TELEPHONE (Include Area Code)	22c. OFFICE SYMBOL	
Lewis Rosado	(513) 255-6519	WRDC/POSL	

(Silicon nitride)

PREFACE

This technical report has been prepared as part of the requirement of the Phase I SBIR Contract No. F33615-89-C-2944 with the AFWAL/POMP, Wright-Patterson Air Force Base, OH. The report covers work conducted during the period August 1989 through February 1990 and constitutes the final report under this contract. The fabrication of self-lubricating surfaces through ion beam assisted deposition and ion implantations, and the necessary characterizations were performed within the Materials Research Division of Universal Energy Systems, Inc., 4401 Dayton-Xenia Road, Dayton, OH 45432. The principal investigator was Dr. Rabi S. Bhattacharya. Dr. A. K. Rai was responsible for electron microscopic analysis. The film deposition, ion implantations and ion beam analyses were performed by A. Smith, W. Lanter and A. W. McCormick, respectively. The friction and wear studies were performed at the High Temperature Materials Laboratory of Oak Ridge National Laboratory under a subcontract to the Martin Marietta Energy Systems, Inc. Dr. C. S. Yust and Mr. C. E. DeVore were responsible for performing friction and wear tests at Oak Ridge.



Accession For	
NTIS CRA&I	<input checked="" type="checkbox"/>
DTIC TAB	<input type="checkbox"/>
Unannounced	<input type="checkbox"/>
Justification _____	
By _____	
Distribution /	
Availability Codes	
Dist	Avail and/or Special
A-1	

TABLE OF CONTENTS

<u>SECTION</u>	<u>PAGE</u>
REPORT DOCUMENTATION PAGE	i
PREFACE	ii
LIST OF ILLUSTRATIONS	iv
1.0 RESEARCH OBJECTIVES	1
2.0 TECHNICAL SUMMARY	1
3.0 RESEARCH WORK CARRIED OUT	2
3.1 Experimental Description	2
3.1.1 Ion Beam Assisted Deposition (IBAD)	2
3.1.2 Substrates	2
3.2 Characterization	3
3.2.1 Composition	3
3.2.2 Microstructure	3
3.2.3 Friction and Wear Tests	4
4.0 RESULTS	5
4.1 RBS Analysis of Surface Composition	5
4.1.1 TiO ₂ Coating	5
4.1.2 CdO Coating	5
4.1.3 Ion Implantation	5
4.1.4 Ti ⁺ + O ⁺ Implanted Si ₃ N ₄ and M50	6
4.1.5 Ag/CaF ₂ /BaF ₂ and CaF ₂ /Ag Coatings	6
4.2 Microstructures	7
4.3 Friction and Wear	8
4.3.1 TiO ₂ Coated and Ti ⁺ + O ⁺ Implanted M50 and Si ₃ N ₄	8
4.3.2 CaF ₂ /Ag on Si ₃ N ₄	9
4.3.3 CdO on M50	9
4.3.4 Wear	10
5.0 ESTIMATE OF TECHNICAL FEASIBILITY	10
5.1 Background	10
5.2 Scale-up	12
6.0 SUMMARY AND CONCLUSIONS	13
7.0 REFERENCES	14

LIST OF ILLUSTRATIONS

<u>FIGURE</u>	<u>PAGE</u>
1	Schematic of IBAD System at UES 15
2	Schematic Diagram of the Controlled Atmosphere, High Temperature Test System. (A) Sphere Used as Pin Member Held in Rod (D). (B) Disc Clamped to Top of Rotating Stage (C). (E) Terminus of Pin Rod and Location of Normal and Tangential Force Transducers. (F) Heating Elements Enclosed Within Quartz Cylinders, the Outer Cylinder (G) Coated with Gold. (H) Insulation at Top and Bottom of Furnace. (I) Water-cooled Plate. (J) Variable Speed Drive Motor. (K) Baseplate for System on Which Enclosure (L) is Seated 15
3	RBS Spectra of TiO ₂ Coating Deposited on a Carbon Substrate with and without an O ₂ ⁺ Beam 16
4	RBS Spectra of CdO Coating Deposited on a Carbon Substrate with and without an O ₂ ⁺ Beam 16
5	Computer Simulation of Depth Distribution (a) 175 keV Ti ⁺ Ions in Steel, (b) 70 keV O ⁺ Ions in Steel 17
6	RBS Spectrum of Ti ⁺ + O ⁺ Implanted Si ₃ N ₄ 18
7	RBS Spectrum of Ti ⁺ + O ⁺ Implanted M50 Steel 18
8	RBS Spectra of As-Deposited and Ion Mixed (1 MeV Ag ⁺) Ag/CaF ₂ /BaF ₂ on Steel 19
9	(a) SAD Pattern and (b) Bright Field Micrograph of TiO ₂ Film Deposited Without Ion Beam 20
10	(a) SAD Pattern and (b) Bright Field Micrograph of Ion Beam Assisted TiO ₂ Film 21
11	(a) SAD Pattern, (b) Bright Field, and (c) Dark Field Micrographs of CdO Film Deposited Without Ion Beam 22
12	(a) SAD Pattern, (b) Bright Field, and (c) Dark Field Micrographs of Ion Beam Assisted CdO Film 23
13	Friction Coefficient (μ) vs Time for M50 Steel with IBAD TiO ₂ Coating and Ti ⁺ + O ⁺ Implantations 24

LIST OF ILLUSTRATIONS (cont'd.)

<u>FIGURE</u>	<u>PAGE</u>
14 Friction Coefficient (μ) vs Time for Si_3N_4 with IBAD TiO_2 Coating and Ti^+ + O^+ Implantations	24
15 Friction Coefficient (μ) vs Time of IBAD CaF_2/Ag Coating on Si_3N_4 at 22°C and 800°C	25
16 Friction Coefficient (μ) vs Time of IBAD CdO Coating on M50 Steel at 22°C and 400°C	25
17 Optical Micrographs of Wear Scars of Si_3N_4 Balls (a) Before, and (b) After the Friction Test on Uncoated Si_3N_4 Disc; (c) Before and (d) After the Test on CaF_2/Ag Coated Si_3N_4 Plate	26
18 Optical Micrographs of Wear Tracks in Si_3N_4 (a) Without and, (b) With CaF_2/Ag Coating	27

1.0 RESEARCH OBJECTIVES

The primary research objective of this work was to develop self-lubricating surface and coatings through direct ion implantations and a combined process of electron beam evaporation and ion implantation. The latter is most commonly referred in the literature as ion beam assisted deposition (IBAD). In IBAD [1-5], the coating material is evaporated by electron beam while bombarding the growing film with energetic ions. The purpose of utilizing ions is to impart kinetic energy and/or chemical activity to materials. Ion energies greater than the threshold displacement energy (~20 eV) of lattice atoms produce recoil lattice atoms. These recoiled lattice atoms can initiate a chain of collisions displacing an even greater number of lattice atoms, causing densification and reduction of stress in the film. When these events occur near the interface of substrate and depositing film, intermixing on an atomic scale takes place providing a strong adherence of the film with the substrate. The initial tasks in Phase I was to establish conditions for ion implantation/IBAD of BaF₂/CaF₂/Ag coatings with Si₃N₄, and CdO, TiO₂ with M50 steel. The final requirement of reaching the overall objective was to examine the modified surfaces for friction and wear at room and elevated temperatures.

2.0 TECHNICAL SUMMARY

The results described in this report indicate that the objectives of this program were clearly met. Ion beam assisted deposition of a bi-layer coating of CaF₂/Ag on Si₃N₄ resulted in a very adherent coating that exhibited significantly low friction and wear characteristic at both room and elevated temperatures (800°C). Ion beam assisted TiO₂ coating on M50 steel showed significantly improved friction and wear characteristics at room temperature. Ion beam assisted CdO coating lowered the friction coefficient of M50 steel at 400°C. The ion beam assisted deposition technique appears to have good technical feasibility for industrial application, owing to the overall simplicity and scalability of the technique.

The details of the experiments and the results of those experiments are described in the following pages. A description of the follow-on work, as well as a more detailed examination

of the ion beam assisted deposition process for various solid lubricants are left to the Phase II proposal that will follow this report.

3.0 RESEARCH WORK CARRIED OUT

3.1 EXPERIMENTAL DESCRIPTION

3.1.1 Ion Beam Assisted Deposition (IBAD)

A schematic representation of our IBAD system is shown in Figure 1. An electron beam evaporation source provides vapor of desired materials which condense on the substrate. A quartz thickness monitor, shielded from the ion beam, measures the deposition rate. A Kaufman type ion gun delivers ions to the depositing substrate. Two small Faraday cups are placed on both sides of the substrate to continuously monitor the current during deposition.

For TiO_2 and CdO depositions, the materials were directly evaporated while bombarding the substrate with O_2^+ ions at an energy of 500 eV. Ar^+ ions were used while depositing CaF_2/Ag layered structure on Si_3N_4 . Also, $\text{Ag}/\text{CaF}_2/\text{BaF}_2$ layers were deposited without the assistance of ion beam but subsequently ion beam mixed using high energy ions.

3.1.2 Substrates

Circular flat discs of 40 mm diameter and 4 mm thickness of both Si_3N_4 and M50 steel were machined to be used as substrates. These discs were used for friction and wear tests in the pin-on-disc machine. A part of the discs were left uncoated/unimplanted to act as a reference for friction and wear tests. In addition, NaCl , graphite and Si (100) wafers were used as substrates for coatings to enable easy characterizations of composition and microstructure.

3.2 CHARACTERIZATION

3.2.1 Composition

Rutherford backscattering (RBS) analysis was used for composition analysis of the deposited coatings. RBS analysis was performed by using the 1.7 MV Tandemron accelerator at UES. In RBS, an incident beam, usually $^4\text{He}^+$ (1-3 MeV), penetrates deep into the sample. A few ions suffer large angle collisions with target nuclei and come back out of the sample. They are detected by a surface barrier detector which can also analyze their energies. The scattering is accurately described by the Rutherford cross section which is proportional to the square of the atomic number of the target atoms. By analyzing the energies of the backscattering particles, one can determine the mass of the target atom. In addition to identifying the mass through kinetics and concentrations through cross sections, one can also determine the depth distribution from a knowledge of energy loss of the projectile to the electrons of the target atoms. This information is generally obtained through experimental measurements and is available in the form of tables. Films deposited on C substrates were used for RBS analysis since both Ti and O or Cd and O signals are separated from the substrate C signals.

3.2.2 Microstructure

Microstructure of the films were determined from Transmission Electron Microscopic (TEM) analysis using the Hitachi H-600 STEM microscope at UES. For quick evaluation of microstructure, some thin ($<100\text{\AA}$) films were deposited on NaCl crystals. The films were then lifted on to carbon coated Cu grids upon dissolving the NaCl substrate in water. Some TEM samples were also prepared from Si substrates by chemical thinning from the backside. For that, $2 \times 2 \text{ mm}^2$ pieces were thinned from the backside using a chemical solution containing HNO_3 , HF and CH_3COOH .

3.2.3 Friction and Wear Tests

The wear experiments were performed in a high-temperature, controlled atmosphere test system. The system utilizes the pin-on-disc wear test geometry and is fitted with a resistance heater furnace capable of providing test temperatures up to 1000°C, Figure 2. The Si_3N_4 and M50 spheres of diameter about 9.5 mm are held in the end of a rod which is fixed in a yoke secured by a support system which includes strain-gauged force transducers. The discs are clamped against a rotation system driven by a variable speed motor. The sphere and disc elements move along a vertical axis and meet within the furnace to form the pin-on-disc configuration. Force transducers provide continuous measurement of both normal and tangential forces, although the values were only recorded periodically for short durations. Load was applied to the pin by dead weight loading.

The test surface of the NBD-100 Si_3N_4 disc specimens were polished by the manufacturer that had a roughness of 0.06 μm or less. The test surface of M50 steel discs were polished by standard metallographic techniques to a roughness $\sim 0.35 \mu\text{m}$. Since the thickness of the ion beam modified surfaces was kept within 1000Å-5000Å only, it was found necessary to minimize the initial contact stress. This was accomplished by flattening M50 steel balls by running on to a Al_2O_3 disc and Si_3N_4 balls by running on a Si_3N_4 disc. A fixed load of 1N was used for 10 minutes at an average sliding velocity of 0.04 m/s. This has resulted in circular wear scars on balls that were subsequently used on the ion beam modified disc surfaces. The average diameter of the flat scar on Si_3N_4 balls was about 460 μm , whereas on M50 steel balls it was about 670 μm . These flattened balls were then run on to both coated and uncoated discs for friction and wear measurements. For these measurements, a normal load of 3N was applied to the flattened ball on disc that was under reciprocating motion at an angular width of 45° on wear track diameters of 20-28 mm. This resulted in a maximum sliding velocity of 0.063 m/s and an average velocity of 0.04 m/s. The average contact pressures for M50 steel and Si_3N_4 under this condition are 8.4 and 18.1 MPa, respectively. Each test was run for 3 minutes. The wear volume measurements of ball specimens was based on the microscopic determination of the circular wear scar diameter which was later converted into wear volume. The disc wear was assessed by surface profilometric measurements across the wear tracks. The room temperature

(23°C) measurements were conducted in laboratory air of ~20% humidity. The high temperature measurements were conducted by first evacuating the chamber by a mechanical pump to about 20 mtorr and then flowing dry nitrogen.

4.0 RESULTS

4.1 RBS ANALYSIS OF SURFACE COMPOSITION

4.1.1 TiO₂ Coating

Figure 3 shows the RBS spectra of TiO₂ coating deposited on a carbon substrate with and without an O₂⁺ beam. The ion beam assisted TiO₂ coating was deposited by using 500 eV O₂⁺ ions at a current density of 150 μA/cm². The stoichiometry and thickness of the TiO₂ films can be evaluated from the spectra. It is found that O/Ti values for the film with and without O₂⁺ ion irradiation are essentially the same. These are 2.25 and 2.19, respectively. The thicknesses are about 3900Å and 3100Å for film with and without ion irradiation.

4.1.2 CdO Coating

Figure 4 shows the RBS spectra of CdO coating with and without ion irradiation. The same ion beam parameters as in the case of TiO₂ coating are used for CdO deposition. The O/Cd ratio for the film with and without O₂⁺ ion irradiation are 0.79 and 0.78, respectively. Again, the ion bombardment does not change the stoichiometry of the film. The thicknesses are about 4800Å and 3000Å for film with and without ion irradiation.

4.1.3 Ion Implantation

Ion implantations were carried out at UES by using the Varian, Extrion 200 kV ion implanter. Since high currents were required for achieving a high dose (concentration), initial efforts were focused in developing the beams in the ion implanter. It was determined that except Ti⁺, O⁺ and Ag⁺, none of the other ions required for this program, e.g., Cd⁺, Ba⁺, and Ca⁺, could

be obtained at a high enough level for achieving a high dose. Thus, ion implantations were carried out only for TiO_2 formation by co-implanting Ti^+ and O^+ ions. 175 keV Ti^+ ions were implanted into M50 steel and NBD-100 Si_3N_4 discs at a dose of $5 \times 10^{16} \text{ cm}^{-2}$ followed by 70 keV O^+ ions at a dose of $1 \times 10^{17} \text{ cm}^{-2}$. A computer simulation of the depth distribution indicates (Figures 5a, b) that the mean range in M50 steel is about 700Å for both Ti^+ and O^+ ions.

4.1.4 $\text{Ti}^+ + \text{O}^+$ Implanted Si_3N_4 and M50

The RBS spectra of $\text{Ti}^+ + \text{O}^+$ implanted Si_3N_4 and M50 are shown in Figures 6 and 7, respectively. The Ti distribution is clearly visible in Si_3N_4 , however, because of proximity of masses between Ti and Fe, Cr, etc., in M50, the signals from implanted Ti is not separated from that of the bulk. The concentration of Ti in Si_3N_4 evaluated from the spectrum agrees with the implanted dose. It should be noted that TiO_2 and CdO coatings were proposed only for M50 steel. However, we decided to examine TiO_2 coating and $\text{Ti}^+ + \text{O}^+$ implantation in Si_3N_4 as well.

4.1.5 Ag/CaF₂/BaF₂ and CaF₂/Ag Coatings

Initially, layers of Ag, CaF_2 and BaF_2 with thicknesses 680Å, 700Å and 1000Å respectively, were sequentially deposited onto Si_3N_4 and M50 steel substrates using electron beam evaporation. The thicknesses were chosen to provide $\text{BaF}_2/\text{CaF}_2$ eutectic composition of about 50/50 mol% and an overall 50/50 wt% composition of Ag and $\text{BaF}_2\text{-CaF}_2$ when homogeneously mixed. This is chosen based on the coating (PS 200) developed by NASA that exhibited excellent friction and wear performance in oxidizing atmosphere up to 900°C and reducing atmosphere up to 760°C.

The deposited films were ion mixed at room temperature using 1 MeV Ag^+ ions at a fluence of $1 \times 10^{16} \text{ cm}^{-2}$. TRIM computer simulation using the actual BaF_2 , CaF_2 and Ag layer thicknesses indicates that the ions should have penetrated through all three layers into the substrate as the calculated mean range (~2560Å) compares well with the total thickness of the layers (2380Å). Figure 8 shows the RBS spectra of unmixed and mixed films on M50 steel substrate. The arrows indicate the energies of particles scattered from surface atoms of Ba, Ag

and Ca. Careful analysis reveals that ion mixing caused a small amount (5-8 at%) of Ag to diffuse out onto the surface. However, the overall mixing between the layers and the layers with the substrate is negligible. Preliminary friction and wear tests of this layered structure revealed a high friction and wear coefficients at room temperature because of the surface layer of BaF₂. This has prompted us to deposit bilayers of CaF₂ and Ag with Ag layer on the surface. These layers were deposited by IBAD process using simultaneous 500 eV Ar⁺ ion bombardment. The thicknesses of CaF₂ and Ag were 1700Å and 680Å, respectively.

4.2 MICROSTRUCTURES

Figures 9a and 9b represent the selected area diffraction (SAD) pattern and the corresponding bright field micrograph of TiO₂ film deposited on NaCl crystal by e beam evaporation of titanium oxide. The presence of diffuse rings in the SAD pattern and the featureless morphology observed in the bright field micrograph are indicative of the amorphous nature of the film.

Figures 10a and 10b show the SAD pattern and the corresponding bright field micrograph of the ion (O₂⁺) assisted TiO₂ film deposited on NaCl substrate. Diffuse rings observed in the SAD pattern confirms the amorphous nature of the film.

Figure 11a represents the SAD pattern of CdO film deposited on NaCl crystal by e beam evaporation of CdO. The diffraction rings observed in the SAD pattern indicate the presence of small crystallites oriented randomly. Careful observation of the SAD pattern showed the presence of two types of diffraction rings namely smooth and spotty rings. The d values of all the diffraction rings were estimated. The estimated value of smooth rings found to match well with that of the known d values of CdO (JCPDS 5-0640), while the d values of most of the spotty rings match well with that of pure Cd (JCPDS 5-0674). From the SAD analysis it was concluded that the present film consists of some randomly oriented crystallites of CdO and of Cd. Diffraction spots superimposed on the smooth diffraction rings were also observed (preferred orientation) in the SAD pattern. Analysis of the diffraction spots indicate that some of the CdO crystallites are oriented along [100]. Figures 11b and 11c show the bright field and dark field

micrographs respectively. The crystallite sizes were estimated from the dark field micrograph to be 60-200Å.

Figure 12a represents the SAD pattern of the ion (O_2^+) assisted CdO film deposited on NaCl crystal. Diffraction rings superimposed with diffraction spots were observed in the SAD pattern. Analysis of the SAD pattern showed that the ring patterns are due to CdO crystallites oriented randomly. Diffraction spots superimposed on the diffraction rings were also observed. Careful analysis of these spots indicated that some of the CdO crystallites are oriented along the following directions [100], [114], [013] and [116]. No indication of pure Cd was found in the SAD pattern. Figures 12b and 12c show the bright field and dark field micrographs respectively. The crystallite sizes were determined from the dark field micrograph to be 60-700Å.

4.3 FRICTION AND WEAR

4.3.1 TiO₂ Coated and Ti⁺ + O⁺ Implanted M50 and Si₃N₄

The friction coefficients as a function of running time was determined at room temperature for all the samples. Each test was repeated from 2 to 3 times. Only a few selected samples were subjected to high temperature tests because of budget limitation.

Figure 13 shows the plot of friction coefficient (μ) as a function of time for M50 steel with IBAD TiO₂ coating and Ti⁺ + O⁺ implanted surfaces. It is clear that Ti⁺ + O⁺ implantation has no effect on the μ , however, TiO₂ coating has significantly reduced the μ for the whole length of the sliding time.

Figure 14 shows the plot of μ as a function of time for Si₃N₄ coated with IBAD TiO₂ coating and Ti⁺ + O⁺ implanted surfaces. IBAD TiO₂ coating considerably reduces the μ , particularly in the beginning of the run, but rapidly decreases afterward; however, the level of μ still stays below the level of uncoated Si₃N₄ on Si₃N₄ throughout the run. The implanted Si₃N₄ showed a higher μ in the beginning, but reduces with time, indicating that there is an effect of implanted Ti⁺ + O⁺ as it is exposed to the surface due to wear of surface layers. Since a high

dose implantation is likely to amorphize the implanted Si_3N_4 layer, we have annealed an implanted sample at 1200°C in high vacuum for 2 hours. The annealing at 1200°C is known to recrystallize the implanted amorphous layers [6]. The annealed layer showed about the same μ as unimplanted Si_3N_4 . This indicates that the reduction in μ in the as-implanted Si_3N_4 may be due to amorphization only and may not be due to the presence of Ti and O or TiO_2 precipitates.

M50 sample coated with IBAD TiO_2 was tested for friction and wear at 800°C . However, in spite of evacuation and backfilling with dry N_2 in the test chamber, the sample surface severely oxidized.

4.3.2 CaF₂/Ag on Si₃N₄

Figure 15 shows μ vs. time of IBAD CaF_2/Ag on Si_3N_4 , both at 22°C and 800°C . The μ in the beginning of the test is 0.1 and 0.2 at 800°C and 22°C respectively as compared to 0.5-0.7 for uncoated Si_3N_4 . The μ at 800°C stayed at about 0.1-0.15 for a considerable length of time, finally reaching a value of about 0.3 at the end of the experiment. However, the room temperature μ monotonically increased to about 0.6 as compared to about 0.8 for uncoated Si_3N_4 . Thus this coating appears to have a great potential for applications covering a wide range of temperature.

4.3.3 CdO on M50

Figure 16 shows the μ vs time of IBAD CdO on M50 both at 22°C and 400°C . Because of earlier experience of severe oxidation of the TiO_2 coated M50 at 800°C , we chose to run CdO coating only up to 400°C . Figure 16 shows that CdO coating indeed has a high μ at room temperature compared to uncoated M50 on M50. However, at 400°C , μ stayed below the level of unmodified M50. Thus, it appears that a composite coating of CdO with Ag or Sn may cover a broad range of temperature for low friction and wear applications.

4.3.4 Wear

Wear was studied by inspecting the wear scars of the balls and wear tracks in the flat plate under the optical microscope. Figures 17a-d show the optical micrographs of wear scars of Si_3N_4 balls before and after the friction tests on Si_3N_4 disc without (17a, b) and with (17c, d) CaF_2/Ag coating. The wear volume can be measured from these wear scars and listed in Table I for the samples tested. The wear of flats could not be determined because of the absence of well-defined groove as measured by surface profilometry and rather high initial surface roughness. It appears that for accurate wear measurements, thicker coating, highly polished surface and prolong friction tests are required. These conditions will be optimized in Phase II. However, optical microscopy was used to qualitatively evaluate the wear of the flat plates. For example, Figures 18a and 18b show the comparison of the wear tracks in Si_3N_4 made by running Si_3N_4 ball without and with CaF_2/Ag coating, respectively. It is clear that the wear track is wider in the uncoated sample compared to the coated sample and the Ag coating in the coated sample is pulled into the center of the track. A careful inspection of Table I reveals that the most significant wear reduction (about a factor of 7) has taken place in the case of CaF_2/Ag coated Si_3N_4 , both at room and elevated temperatures. The next noticeable effect is a factor of 2 reduction in wear in the TiO_2 coated M50 steel.

5.0 ESTIMATE OF TECHNICAL FEASIBILITY

5.1 BACKGROUND

Ion implantations and a number of coating deposition methods are already in use in many different applications of surface treatments. Spire Corporation is already treating space shuttle engine bearings made of 440-C steel to improve the wear resistance. The use of directed ion beams to treat surfaces may incur higher cost than the conventional coating technology, however, the higher cost can be justified by the benefits of this technology. The same can be said about the ion beam assisted deposition which may even be less costly than the direct ion implantation. The practical requirements of the ion implantation and ion beam assisted deposition processes, such as the need for a vacuum chamber, ion beam source and sample manipulator assemblies are

TABLE 1. Wear Volumes of Balls.

FLAT DIA. (μm)	FLAT AREA (μm^2)	SPHERE RADIUS (μm)	TOTAL SPHERE WEAR VOL. (mm^3)	WEAR VOL. (mm^3)	COATING/SUBSTRATE
447	1.57E-07	4763	4.12E-04		
481	1.82E-07	4763	5.52E-04	1.40E-04	TiO ₂ /Si ₃ N ₄
433	1.47E-07	4763	3.63E-04		
485	1.85E-07	4763	5.71E-04	2.08E-04	Ti+O/Si ₃ N ₄
428	1.44E-07	4763	3.46E-04		
461	1.67E-07	4763	4.66E-04	1.20E-04	Ti+O/Si ₃ N ₄
409	1.31E-07	4763	2.89E-04		
466	1.71E-07	4763	4.86E-04	1.98E-04	Ti+O/Si ₃ N ₄
447	1.57E-07	4763	4.12E-04		
481	1.82E-07	4763	5.52E-04	1.40E-04	Si ₃ N ₄
428	1.44E-07	4763	3.46E-04		
433	1.47E-07	4763	3.63E-04	1.65E-05	CaF ₂ -Ag/Si ₃ N ₄
461	1.67E-07	4763	4.66E-04		
466	1.71E-07	4763	4.86E-04	2.05E-05	CaF ₂ -Ag/Si ₃ N ₄
668	3.50E-07	4763	2.06E-03		
702	3.87E-07	4763	2.51E-03	4.52E-04	Ti+O/M50
673	3.56E-07	4763	2.12E-03		
702	3.87E-07	4763	2.51E-03	3.90E-04	M50
490	1.89E-07	4763	5.95E-04		
576	2.61E-07	4763	1.14E-03	5.41E-04	M50
678	3.61E-07	4763	2.18E-03		
711	3.97E-07	4763	2.64E-03	4.57E-04	Ti+O/M50
678	3.61E-07	4763	2.18E-03		
697	3.82E-07	4763	2.44E-03	2.55E-04	TiO ₂ /M50
740	4.30E-07	4763	3.10E-03		
754	4.47E-07	4763	3.34E-03	2.41E-04	TiO ₂ /M50
500	1.96E-07	4763	6.45E-04		
524	2.16E-07	4763	7.78E-04	1.33E-04	TiO ₂ /Si ₃ N ₄
462	1.68E-07	4763	4.70E-04		
481	1.82E-07	4763	5.52E-04	8.22E-05	Ti+O/Si ₃ N ₄ Annealed
476	1.78E-07	4763	5.30E-04		
481	1.82E-07	4763	5.52E-04	2.26E-05	CaF ₂ -Ag/Si ₃ N ₄ 800°C
				4.71E-04	CdO/M50
				2.02E-04	CdO/M50, 400°C

essentially identical to existing industrial methods. This suggests a high practical feasibility of ion implantation and ion beam assisted deposition on an industrial side. Since the Phase I research showed promising results with ion beam assisted coatings, we will review the technical aspects of this process in terms of practical feasibility.

5.2 SCALE-UP

There is no inherent limitation of scaling-up the ion beam assisted deposition process. Very large diameter ion beam sources have been built with total beam currents of several tens of amperes. Specifications for a moderate scale-up design are listed below:

Ion Source

The largest diameter ion gun manufactured by the Commonwealth Scientific, Inc. is 38 cm diameter.

Beam Current = 1 amp

Beam Voltage = 150 eV - 1.5 keV

Vacuum Chamber

8 feet diameter and 8 feet tall with two electron guns.

Operation

Coating Thickness = 3 μm

Deposition Time = 60 minutes

Surface Area = 1130 cm^2

Production

Assuming 90% yield, coated area per hour = 1017 cm²

Surface area coated per year assuming 2000 hours/year of operation = 2.03x10⁶ cm²

Cost

Operating Cost per Year = \$500,000

Cost per cm² = \$0.25

The cost estimate includes direct and indirect costs of equipment, floor space, labor, materials and utilities.

In conclusion, ion beam assisted deposition of self lubricating coatings appears to have high technical feasibility even with a moderate scale-up.

6.0 SUMMARY AND CONCLUSIONS

The purpose of this work was to study the feasibility of tribological surface modifications through ion beam and vapor depositions. The surfaces considered in Phase I were M50 steel and Si₃N₄-NBD100, and modifications considered were ion beam assisted TiO₂, CdO and CaF₂/Ag coatings, and co-implantations of constituent elements to form the above compounds beneath the surface. Ion beam assisted TiO₂ coating significantly reduces the friction and wear of M50 steel. This coating is also effective in Si₃N₄, but for a shorter length of time. Ion beam assisted CdO on M50 shows high friction at room temperature but lower friction at elevated temperature (400°C). The best coating, however, is the CaF₂/Ag on Si₃N₄ which shows low friction and wear from room to high (800°C) temperatures. In fact, the friction coefficient at 800°C reduces to about 0.1 for Si₃N₄ on Si₃N₄ with the above coating. The fact that very adherent solid lubricating coatings can be fabricated by ion beam assisted deposition points to many promising practical applications. A program to systematically develop this process for defense and aerospace applications is outlined in the Phase II proposal that will follow this report.

7.0 REFERENCES

1. C. Weissmantel, Thin Solid Films 58 (1979) p. 101.
2. L. Pranevicius, Thin Solid Films 63 (1979) p. 77.
3. G. A. Al-Jumally, S. R. Wilson, A. C. Barron, J. R. McNeil, and B. L. Doyle, Nucl. Instr. and Meth. Phys. Res. B7/8 (1985) p. 906.
4. P. J. Martin, R. P. Netterfield, W. G. Sainty, G. Clark, W. A. Langford, and S. H. Sie, Appl. Phys. Lett. 43 (1983) p. 711.
5. F. E. E. Baglin and G. Clark, Nucl. Instr. Meth. in Phys. Res 7/8 (1985) p. 881.
6. R. S. Bhattacharya, A. K. Rai, and P. P. Pronko, J. Appl. Phys. 61 (1987) 4791.

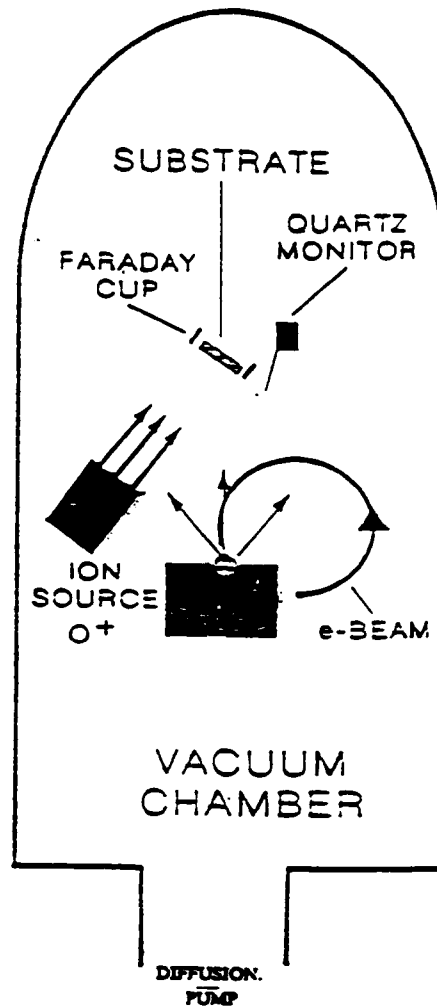


Figure 1. Schematic of IBA Deposition System at UES.

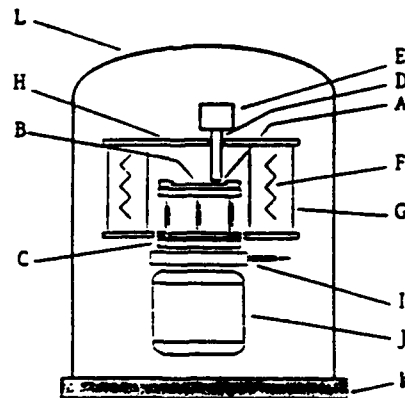


Figure 2.

Schematic Diagram of the Controlled Atmosphere, High Temperature Test System. (A) Sphere Used as Pin Member Held in Rod (D), (B) Disc Clamped to Top of Rotating Stage (C), (E) Terminus of Pin Rod and Location of Normal and Tangential Force Transducers, (F) Heating Elements Enclosed Within Quartz Cylinders, the Outer Cylinder (G) Coated with Gold, (H) Insulation at Top and Bottom of Furnace, (I) Water-cooled Plate, (J) Variable Speed Drive Motor, (K) Baseplate for System on Which Enclosure (L) is Seated.

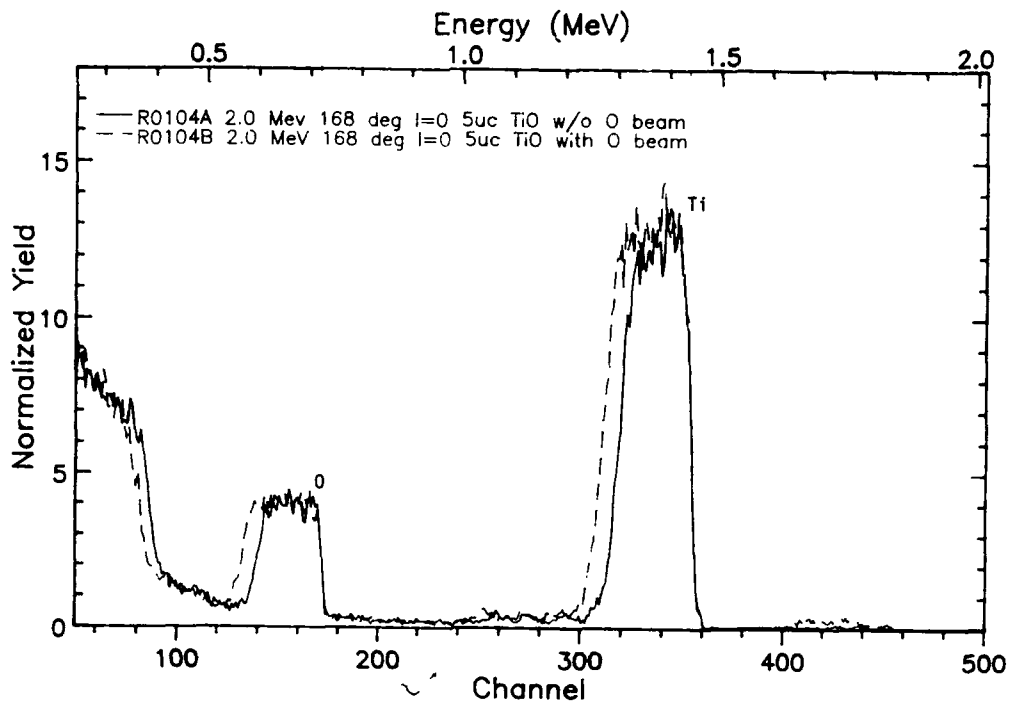


Figure 3. RBS Spectra of TiO₂ Coating Deposited on a Carbon Substrate with and without an O₂⁺ Beam.

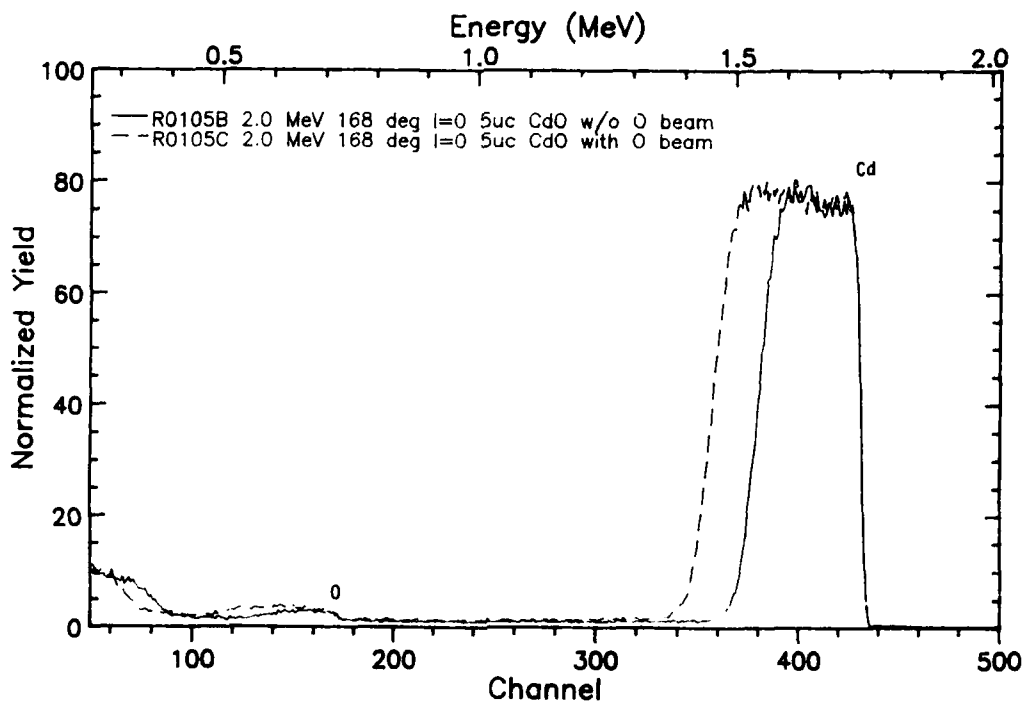


Figure 4. RBS Spectra of CdO Coating Deposited on a Carbon Substrate with and without an O₂⁺ Beam.

TAM-88

Ion - Ti 48 175 keV

Target 1- steel -7.87 g/cm³

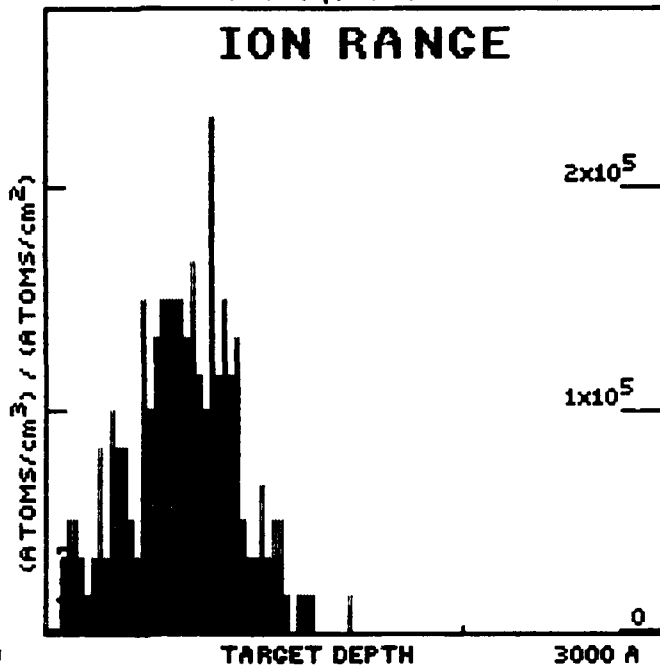
Layers 2-
3-

Ion Number : 201
Ion Energy : 4 eV
Cascade E : 0 eV
Backscatter: 0
Transmit. : 0

AVERAGES
Mean Range : 653 A
Stragglng : 264 A
Vac./ Ion : 2020

ENERGY LOSS (%)
IONS RECOILS
Ioniz.: 24.7 19.7
Vac. : 1.1 21.8
Phon. : .4 32.5

Command: SB, E, R, P, p, C, N, F2 Version - 4.1



(a)

TAM-88

Ion - O 16 70 keV

Target 1- steel -7.87 g/cm³

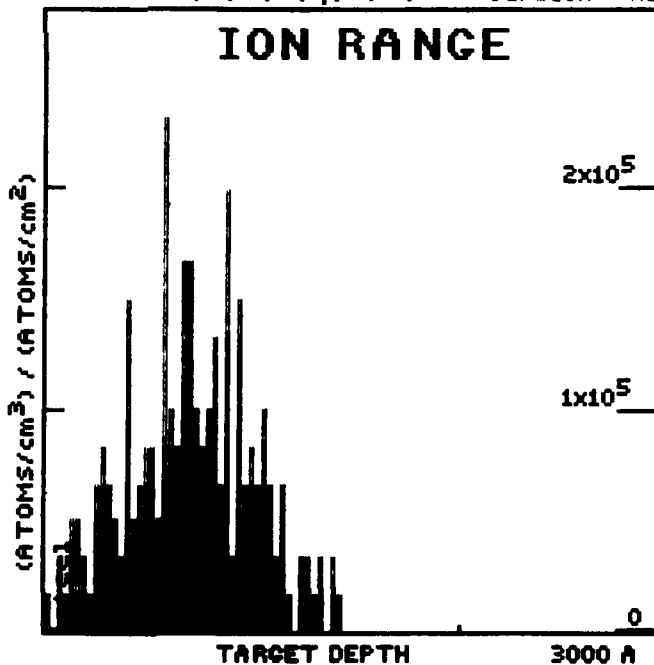
Layers 2-
3-

Ion Number : 201
Ion Energy : 2 eV
Cascade E : 0 eV
Backscatter: 3
Transmit. : 0

AVERAGES
Mean Range : 704 A
Stragglng : 304 A
Vac./ Ion : 591

ENERGY LOSS (%)
IONS RECOILS
Ioniz.: 51.6 9.5
Vac. : 2 14.7
Phon. : 1 21.4

Command: SB, E, R, P, p, C, N, F2 Version - 4.1



(b)

Figure 5. Computer Simulation of Depth Distribution (a) 175 keV Ti⁺ Ions in steel, and (b) 70 keV O⁺ Ions in Steel.

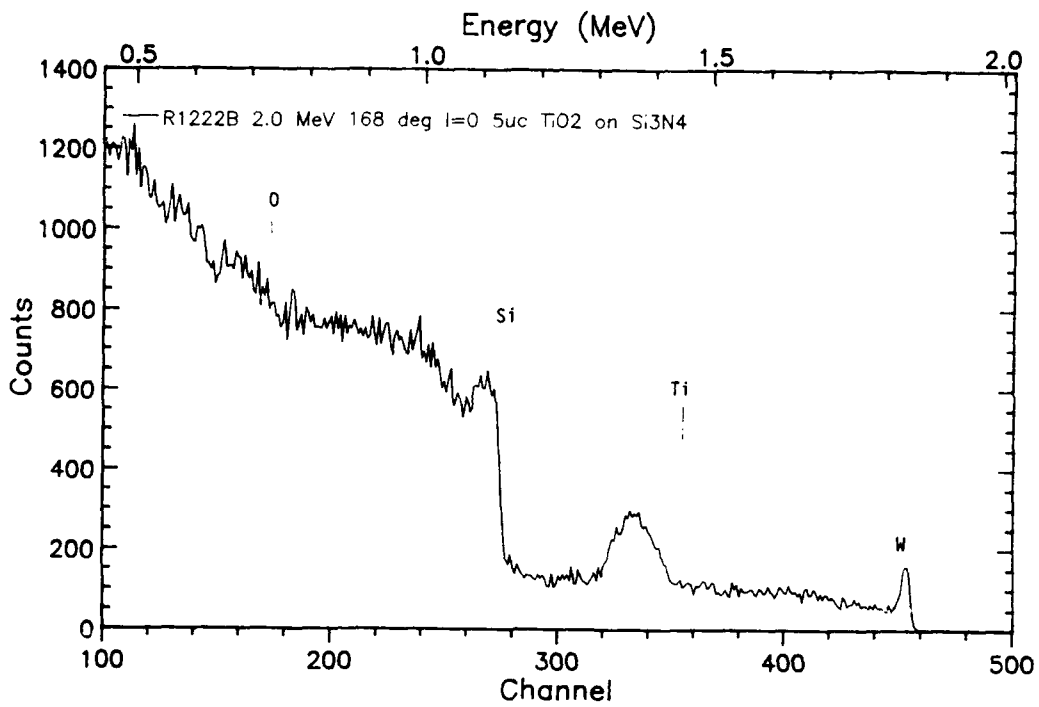


Figure 6. RBS Spectrum of Ti⁺ + O⁺ Implanted Si₃N₄.

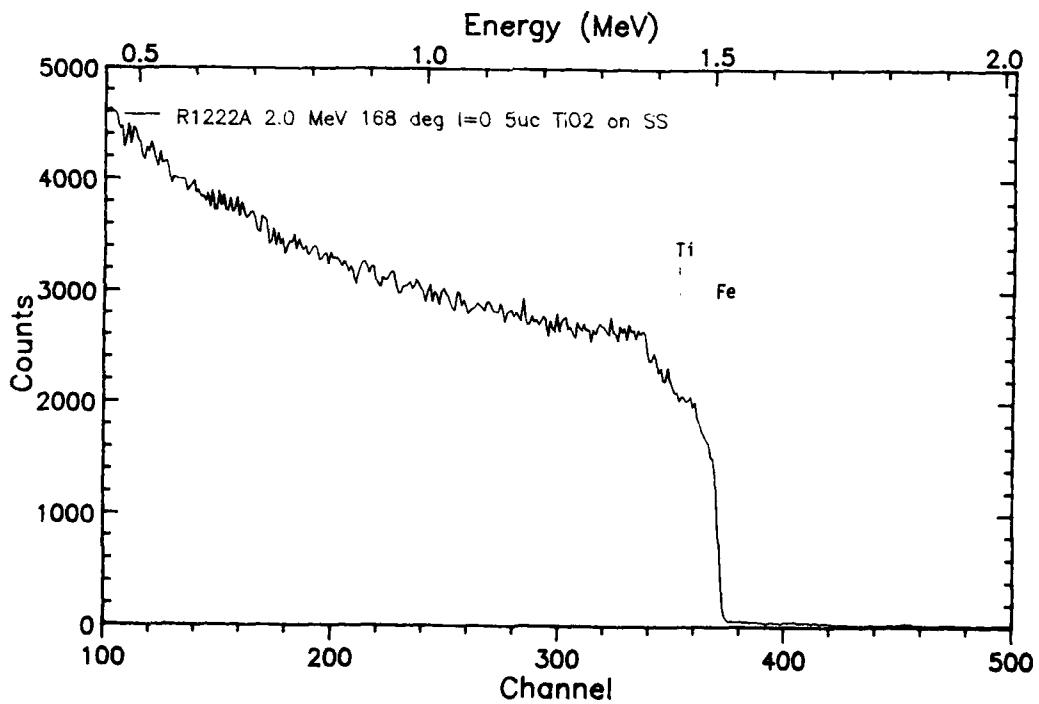


Figure 7. RBS Spectrum of Ti⁺ + O⁺ Implanted M50 Steel.

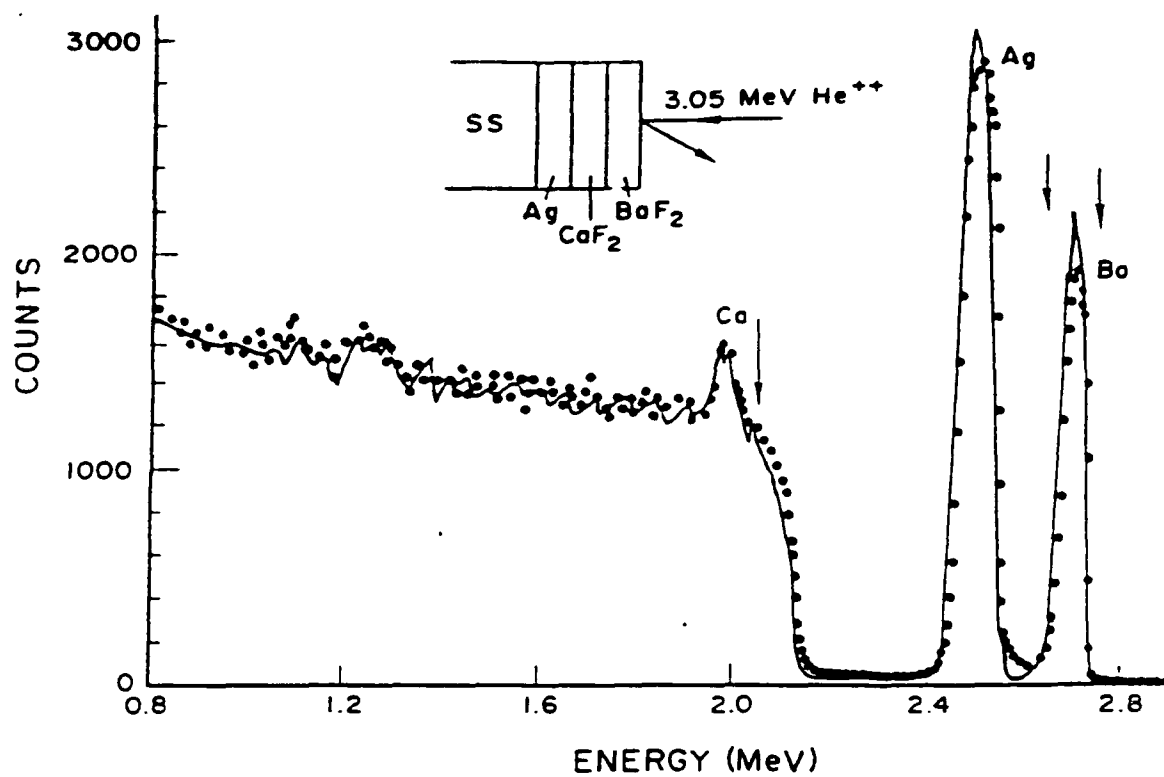
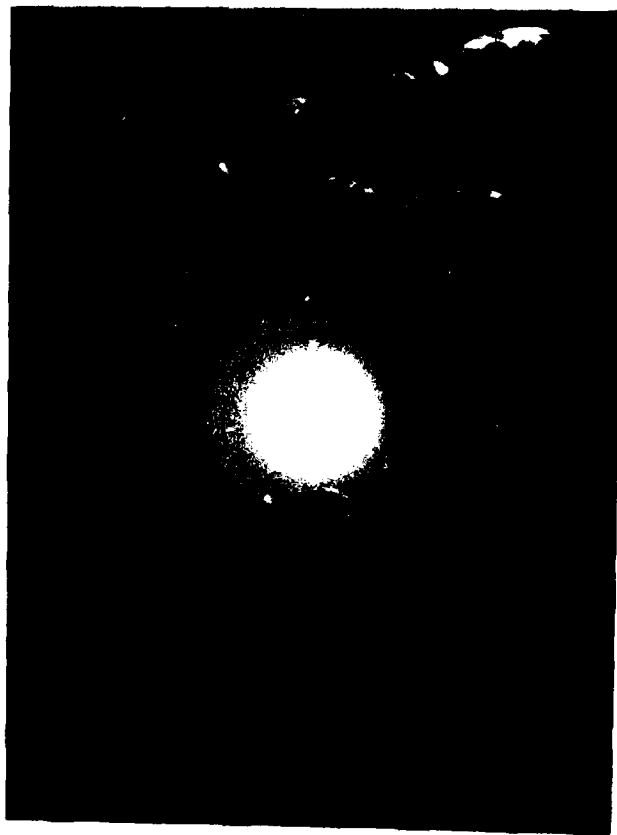


Figure 8. RBS Spectra of As-Deposited and Ion Mixed (1 MeV Ag⁺) Ag/CaF₂/BaF₂ on Steel.



a



b

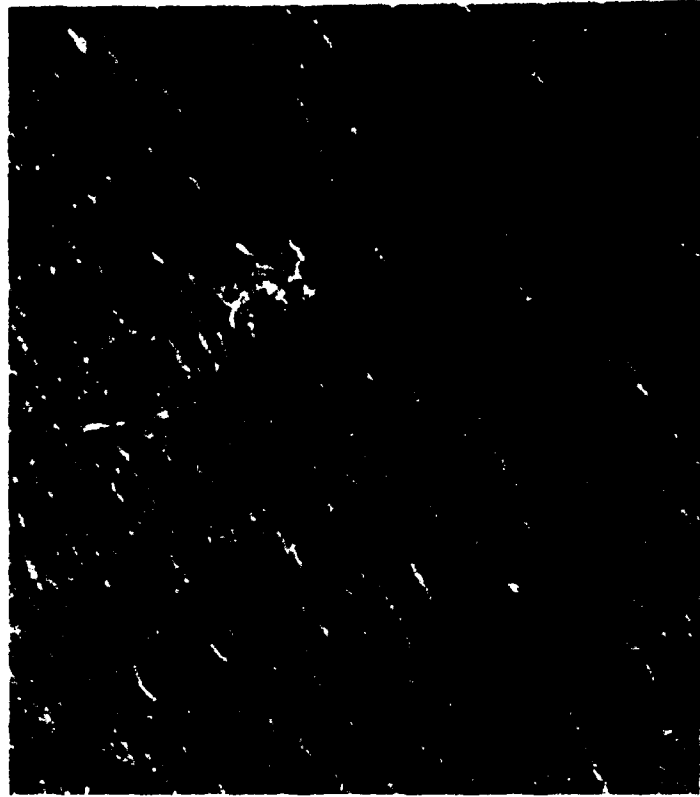
0.07 μ m



Figure 9. (a) SAD Pattern and (b) Bright Field Micrograph of TiO_2 Film Deposited Without Ion Beam.



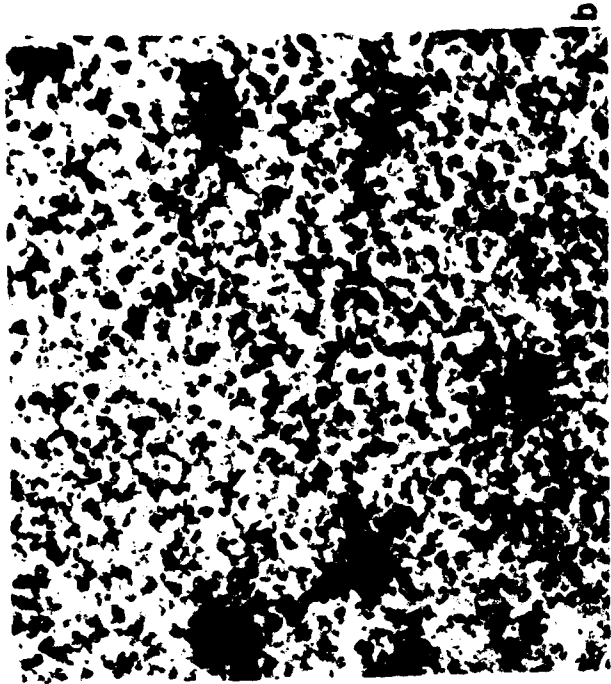
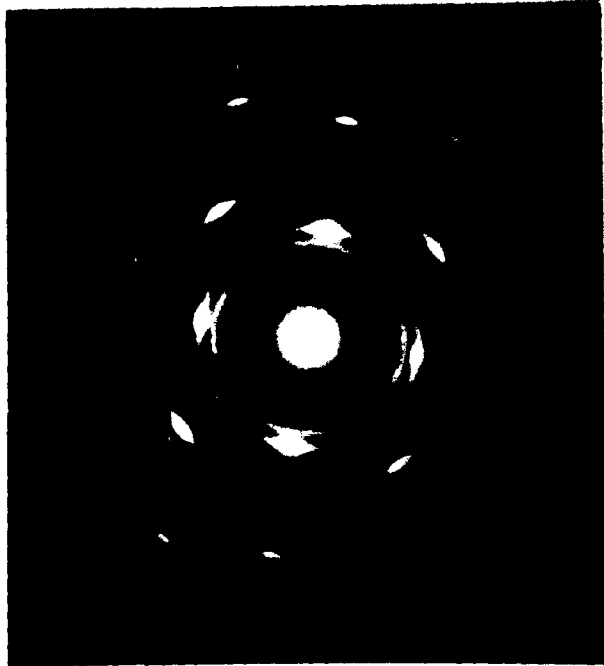
d



b

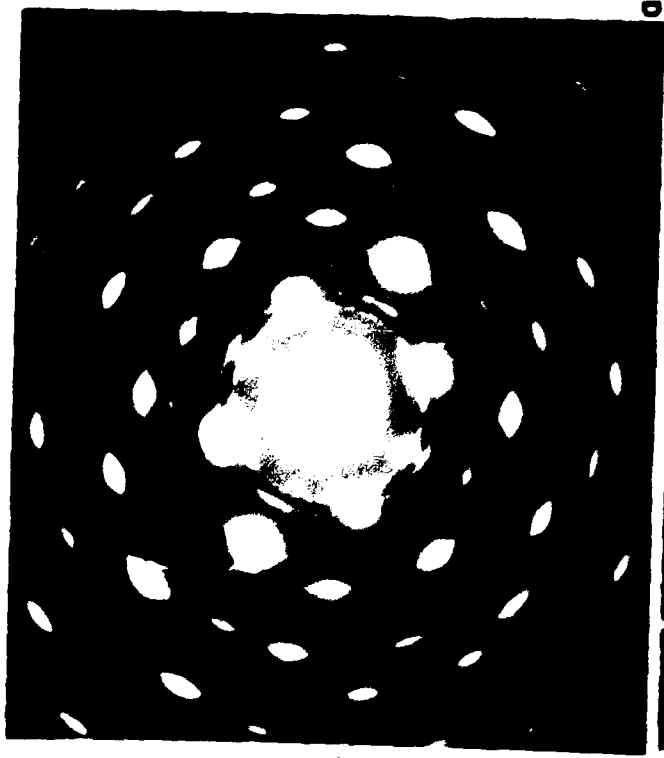
0.1 μ m

Figure 10. (a) SAD Pattern and (b) Bright Field Micrograph of Ion Beam Assisted TiO₂ Film.

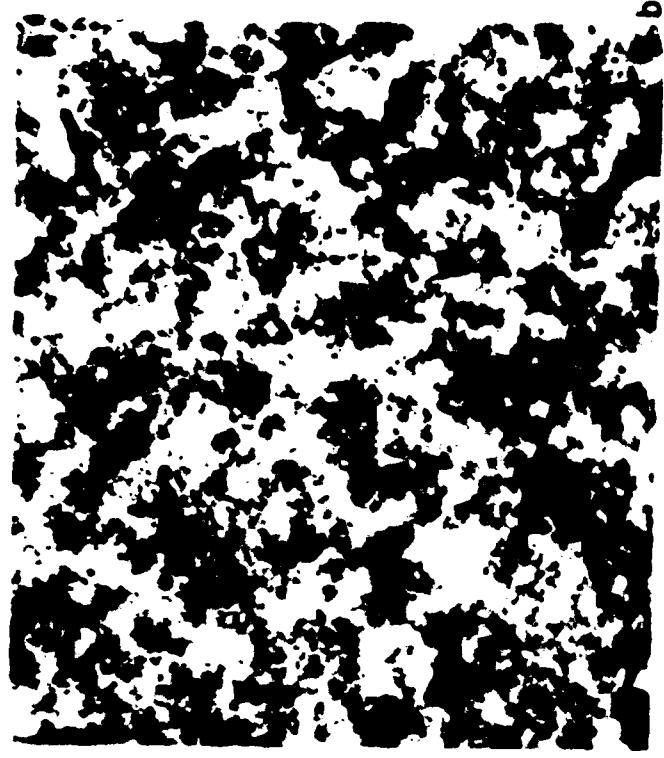


0.1 μ m

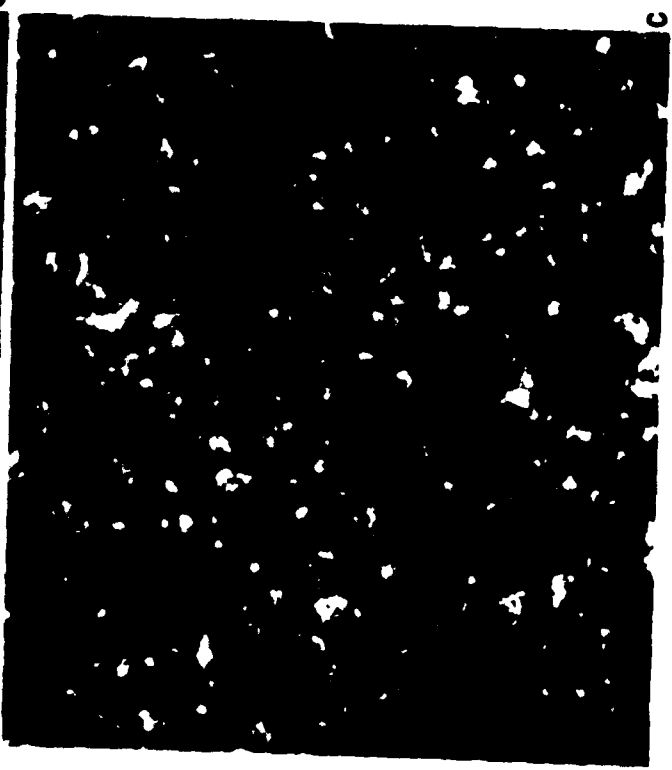
Figure 11
(a) SAD Pattern, (b) Bright Field and (c) Dark Field
Micrographs of CdO Film Deposited Without Ion
Beam.



a



b



c

0.1 μ m

Figure 12. (a) SAD Pattern, (b) Bright Field and (c) Dark Field Micrographs of Ion Beam Assisted CdO film.

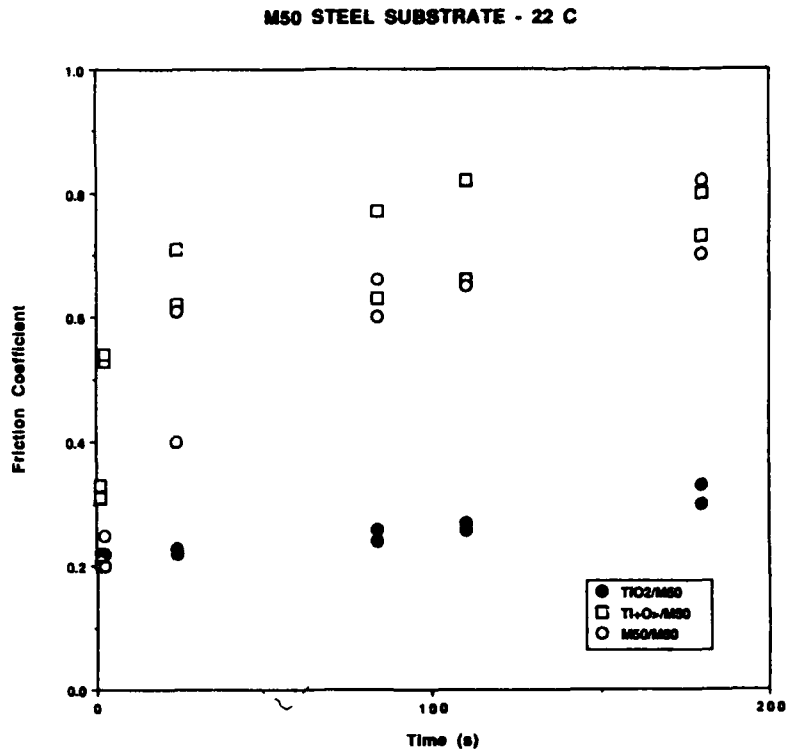


Figure 13. Friction Coefficient (μ) vs Time for M50 Steel with IBAD TiO_2 Coating and $\text{Ti}^+ + \text{O}^+$ Implantations.

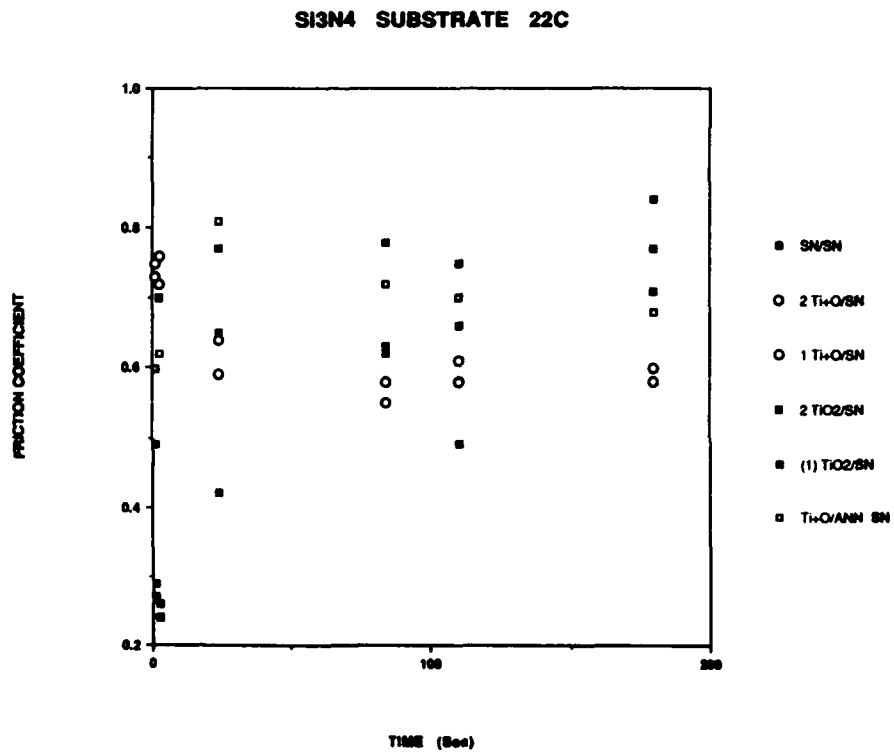


Figure 14. Friction Coefficient (μ) vs Time for Si_3N_4 with IBAD TiO_2 Coating and $\text{Ti}^+ + \text{O}^+$ Implantations.

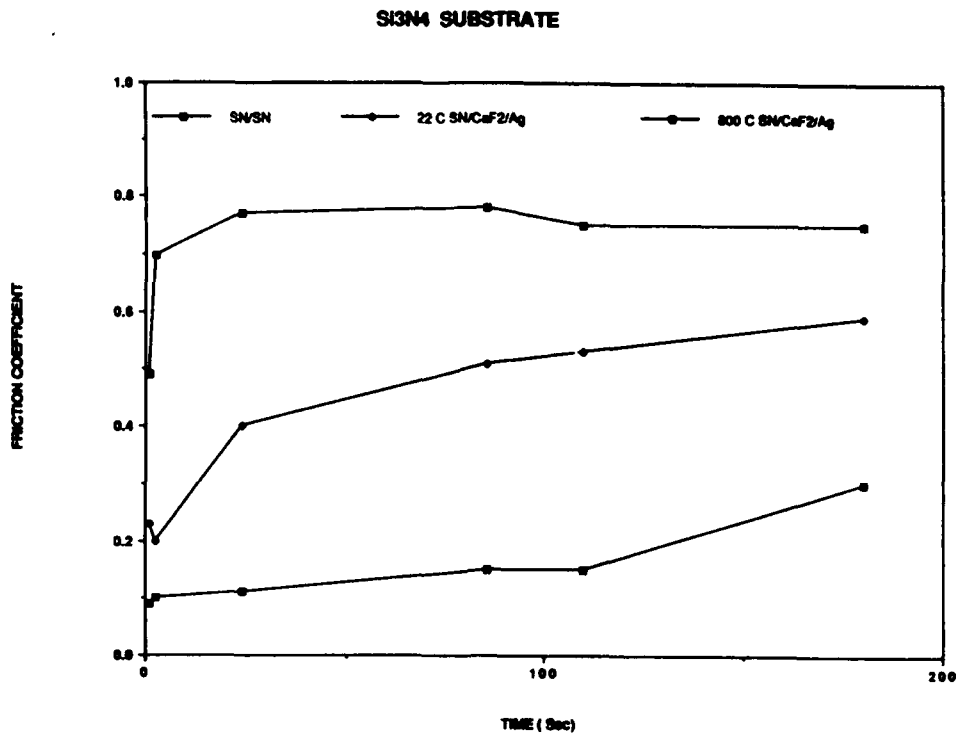


Figure 15. Friction Coefficient (μ) vs Time of IBAD CaF_2/Ag Coating on Si_3N_4 at 22°C and 800°C .

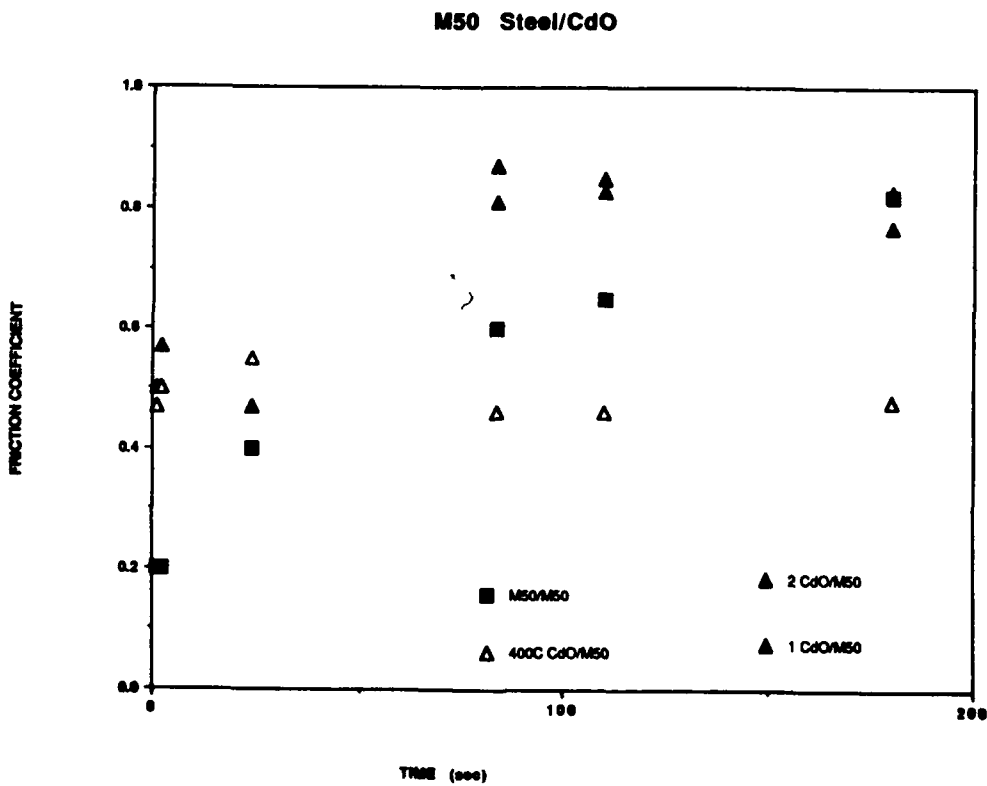
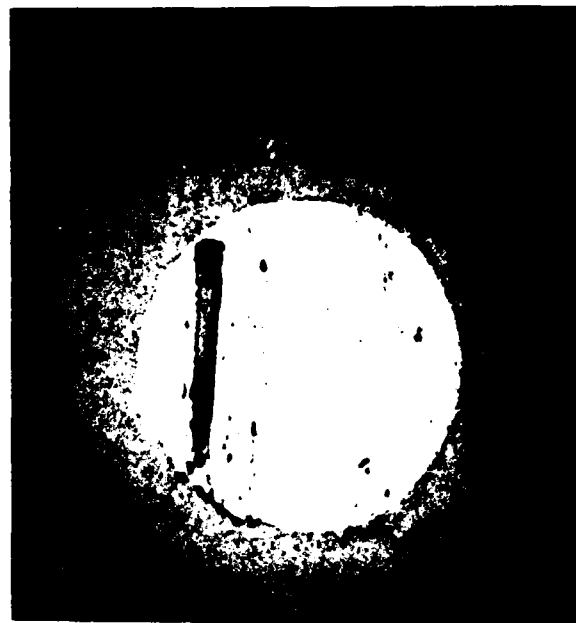


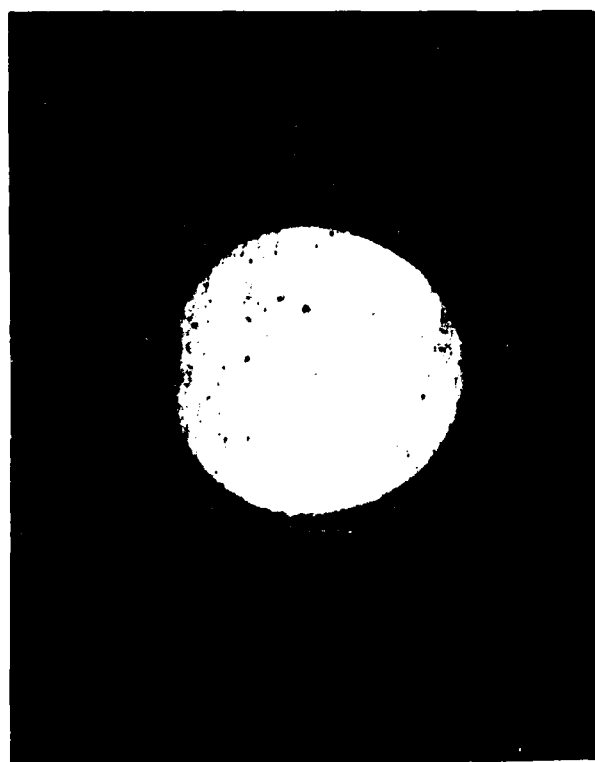
Figure 16. Friction Coefficient (μ) vs Time of IBAD CdO Coating on M50 Steel at 22°C and 400°C .



a



b



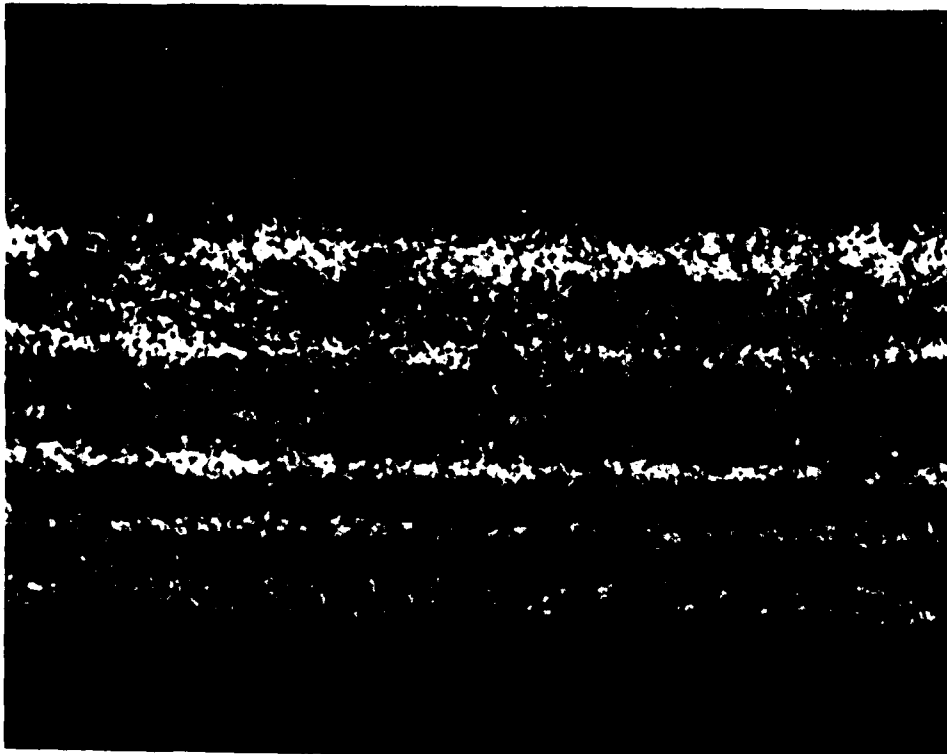
c



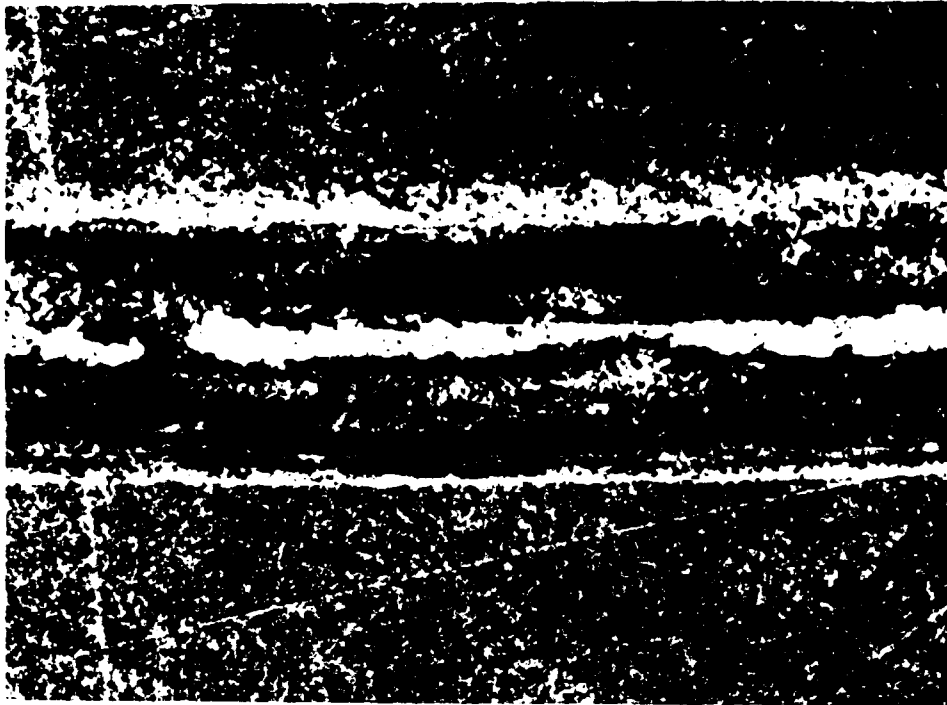
d

104X

Figure 17. Optical Micrographs of Wear Scars of Si_3N_4 Balls (a) Before, and (b) After the Friction Test on Uncoated Si_3N_4 disc; (c) Before and (d) After the Test on CaF_2/Ag Coated Si_3N_4 Disc..



A



B

Figure 18. Optical Micrographs of Wear Tracks in Si_3N_4 (a) Without, and (b) With CaF_2/Ag Coating.